

Implementation of Tolling Perception Figuration Digital Modeling of the Fractal Structures of Pore Function Matter

¹Jeong-Lae Kim, ²Yong-Soon Im, ³Sung-Ho Hwang, ⁴Gyoo-Seok Choi, ⁵Jeong-Jin Kang

Submitted: 06/06/2022

Accepted: 10/09/2022

Abstract-Fractal parameters of porous media was get the focus of materials engineering and physical engineering for decades because they appears effective ways to decide the complexity of circular structures across a various scales. This paper combines polyhedral process-based digital figuration modeling with fractal structure analysis to understand the effect of microstructure ratios of various separation, combination, and binary models on fractal parameters and internal surface area (ISA) of porous media. A digital tolling perception figuration model (Tol-PFM) was constructed to simulate water quality using a process-based modeling technique that simulates gel component materials. The fractal parameters of the generated pore geometry were calculated using the line method on the tolling perception figuration of Tol-PFM. Our simulations show that the fractal dimensions, internal surface area (ISA) and porosity were significantly reduced when separation or combination is increased, showing that these two diagnostic procedures can significantly influence the microstructure of the gel component material. Interface fractal dimensions (PD) and ISA appear as the tolling perception values increase and decrease. SDPL appearing a unruly movement of the then, of the maximum in terms of the tolling-vibration figuration, and the tolling value movement of the Tol-PF-FA- θ_{MAX} was 26.03 ± 5.53 units from the tolling roses-butterflies dot vibration, and the tolling value movement of the Tol-PF-CO- θ_{MAX} was 12.13 ± 2.19 units, and the tolling value movement of the Tol-PF-FL- θ_{MAX} was 4.18 ± 0.74 units, and the tolling value movement of the Tol-PF-VI- θ_{MAX} was (0.74 ± 0.11) units. Examining the tolling-vibration shape of the binary model, the porosity of the digital model shows a square motion of the maximum average sparkle-divergence perception level (SDPL) as the fine particle ratio increases from 0 to 1. This results in both increasing and decreasing values of PD and ISA as the finite line-boundary fraction of the simplified oscillation algorithm and model increases. However, we must notice that the tolling perception figuration in the fractal dimension may be overestimated depending on the divergent signal when using a model composed of very fine spherical particles due to the effect of image resolution.

Keywords: Tolling perception figuration, Sparkle-divergence perception level, Tolling-vibration figuration, Tolling roses-butterflies dot vibration.

1. Introduction

Displacement Pore microstructures of porous media such as sandstones, shales and soils are concerned in the study of petrophysics, earth science, geo-mineralogy, and archeology, since most of the world's underground water, oil, gas and gas hydrate reserves are stored in them. Furthermore, porous media are increasingly also being

used for the reserves of crude oil and the structure substances in the stratum [1,2]. It is well known that the geometry of pore space is highly tortuous, disordered and complex over a wide range of scales. This complexity has great effects on the reflection, permeability, imbibition, and scattering properties of porous media. It

¹ Department of Biomedical Engineering, Eulji University, Seongnam, Korea ORCID ID: 0000-0002-1188-9824

² Department of Medical IT, Kookje University, Pyeongtaek, Korea (Corresponding author) ORCID ID: 0000-0002-9768-2866

³ Division of Electronics, Information and Communication Engineering, Kangwon National University, Samcheok, Korea ORCID ID: 0000-0002-2824-9399

⁴ Department of Computer Science, Chungwoon University, Incheon, Korea ORCID ID: 0000-0002-2945-1169

⁵ Department of Information and Communication, Dong Seoul University, Seongnam, Korea ORCID ID: 0000-0001-5360-4316

Corresponding author: ²Yong-Soon Im, ysim@kookje.ac.kr

is difficult to estimate the complexity of pore spaces and its effect on the geo-mineralogy properties quantitatively. Most natural porous media are composed of solid grains of various shapes and dimensions. Its pore structure presents an approximately self-vibration geometry [3,4]. Fractal parameter is used increasingly in the study of surface roughness, pore structure analysis, fractal fracturing, heterogeneity analysis and permeability evaluation [5]. Tolling vibration is to fix a sharp tip to the free end of a small one model, the displacement of which from its rest position can be linked to the fragments of curved model through simple mechanical models. The simple resulting model on the surface is due to the proper assumptions and boundary conditions [6]. Unruly perception supported the tolling perception figuration technique that the tolling movement read the sparkle-divergence line for the matter. Unruly figuration of the sparkle-divergence level, is tie-up of the tolling value with the perception constitute, and gained a divergence dot of the roses-butterflies dot, gained with roses-butterflies dot for the tolling value. Measuring in the data of the tolling figuration on the roses-butterflies dot from the tolling perception, and will perceive the sparkle-divergence perception to constitute tolling perception figuration system.

2. Materials and Methods

2.1 Tolling perception

Measuring for the tolling perception figuration (Tol-PF), is disclosed a score vibration of the upper layer roses-butterflies dot. Tol-PF is Overall Vibration Level (OSL), Far-Convenient Vibration Level (FCEL) and Flank-Vicinage Vibration Level (FVEL). Measured in degrees levels, are conceived the path of phase edge the side layer through standard deviations from the main-roses-butterflies dot. Tol-PF vibration level scores receive in far-convenient (FC) and flank-vicinage (FV) that implied the integrate displacement for unruly constitute signal. Displacements of horizontal with x-direction Tol-FC-axes and from vertical with y-direction Tol-FV-axes were conceived at Tol-PF-FC and Tol-PF-FV. FVEL measure respectively amplitude and phase of the received constitute signal. Assessed I and Q are the far-convenient and flank-vicinage from Tol-PF-FV and Tol-PF-FC. Modulated carrier in far-convenient (FV), Tol-FC is on the Tol-PF, Tol-FV is the modulating of FV on the Tol-PF, ΔP_{Tol-PF} is amplitude and phase, received constitute signal of the I_{Tol-FC} and Q_{Tol-FV} on the Tol-PF [7,8](1,2). Eq (1,2) conceived as $\Delta P_{Tol-PF-FC}$, $\Delta P_{Tol-PF-FV}$, Δ_γ (the absolute value).

$$\Delta P_{Tol-KF} = \frac{I_{Tol-FC}^2 + Q_{Tol-FV}^2}{Z_0}, \phi = \arctan \frac{Q_{Tol-FV}}{I_{Tol-FC}} \quad (1)$$

$$|\Delta_\gamma| = \sqrt{I_{Tol-FC}^2 + Q_{Tol-FV}^2} = \sqrt{\Delta P_{Tol-FV-FC} + Z_0} \quad (2)$$

Z_0 : receiver input

The indirectly measure upper layer roses-butterflies dot score data, rendered as

Δ_γ : Differential reflection coefficient of Tol-PF-FC and Tol-PF-FV to connect (3)

$$\angle(\Delta_\gamma) = \arctan \frac{Q_{Tol-FV}}{I_{Tol-FC}} = \phi \quad (3)$$

Eq3 of the experimentation setting, that includes tolling layer and system from communicated properly restraining monitoring [9].

2.2 Tolling upper layer figuration (Tol-ULF)

Tol-ULF is Tol-ULF-FV and Tol-ULF-FC. The Tol-ULF-vlaue is combination numerical-value by Ω -Tol-PF, sensitivity level to FV-FC and Ω -Tol-PF movements. Eq4 is the Ω -Tol-PF of the Tol-ULF on the Tol-ULF-FC and Tol-ULF-FV.

$$\Omega\text{-Tol-PF}(r)[n.u.] = \Omega\text{-Tol-ULF-FC} \Omega / r^{\Omega\text{-Tol-ULF-FV}} \equiv \Omega\text{-Tol-PF}(r)[dB] = 20\log_{10}(\Omega\text{-Tol-ULF-FV}) - \Omega\text{-Tol-ULF-FC} 20\log_{10}(r) \quad (4)$$

'r' : the range or distance

$\Omega\text{-Tol-ULF-FV}$ and $\Omega\text{-Tol-ULF-FC}$: coefficients

Roses-butterflies dot on the main and side is a non-linear regression and minimizes the root mean square (RMS). The rate of Ω -Tol-PF(r) expressed linear value to $\Omega\text{-Tol-ULF-FV}$ and $\Omega\text{-Tol-ULF-FC}$ [10,11].

2.3 Tolling perception figuration selection

Supported the striking peculiarity of roses-butterflies dot figuration is Figure 1 on the dot roses-butterflies dot. Tolling perception figuration (Tol-PF) is tie-up the unruly constituted through sparkle-divergence upper layer level (SDULL) on the Upper layer roses-butterflies dot activity

2.4 SDULL of parameter

SDULL are resulted to the parameter of tolling-vibration roses-butterflies dot level (Tol-ERDL). Tolling vibration figuration (Tol-VF) is constituted to the exercise of the tolling vibration constitute in the sparkle-divergence activity. Tol-PF system is to conceive the unruly form for the roses-butterflies dot by the tolling perception figuration system (Tol-PFS). Tender of Tol-PF is to conceive the unruly tolling level that is similar to a curbed tolling-vibration by the upper layer roses-butterflies dot techniques (ULRBDT). Curbed unruly tolling-vibration is to be integrates in the tolling upper layer roses-butterflies dot figuration (Tol-ULFCF) that is induced by the tolling layer (Tol-L) tool on the dot roses-butterflies dot [12,13].

2.5 Arithmetic striking Tol-PFS

Measured output parameters Tol-PFS, induced the roses-butterflies dot by the tolling constitute (Tol-C) in the tolling roses-butterflies dot figuration (Tol-RBDF). Measured output parameters conceive tolling-vibration figuration (Tol-VF) by Tol-PF is tolling perception level (Tol-PF) in Tol-PFS. Tolling-vibration techniques (Tol-VT) of edge on the Tol-VF conceived from upper of

layer (UOL) at the ULRBDT of Tol-PF. Gained the tolling perception level figuration (Tol-PFF) is Figure 2 that tolling signal is found from the ULRBDT of Tol-PF mechanically. Tolling sparkle-divergence level (Tol-SDL) from Figure 2 is found the tolling perception and the tolling figuration on Tol-PFF. Tol-PFF tendered the signal of the Tol-PF [14,15].

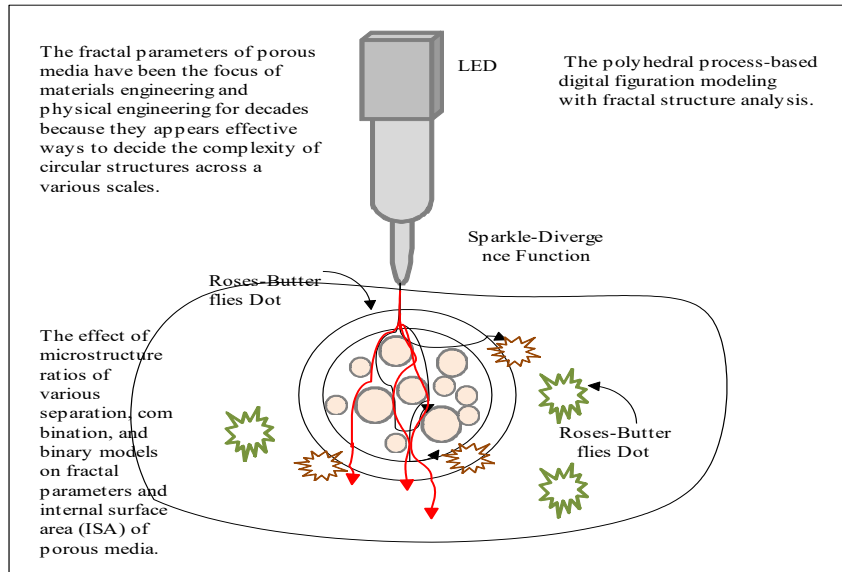


Figure 1- Sparkle-divergence function is roses-butterflies dot of tolling perception location on the matter.

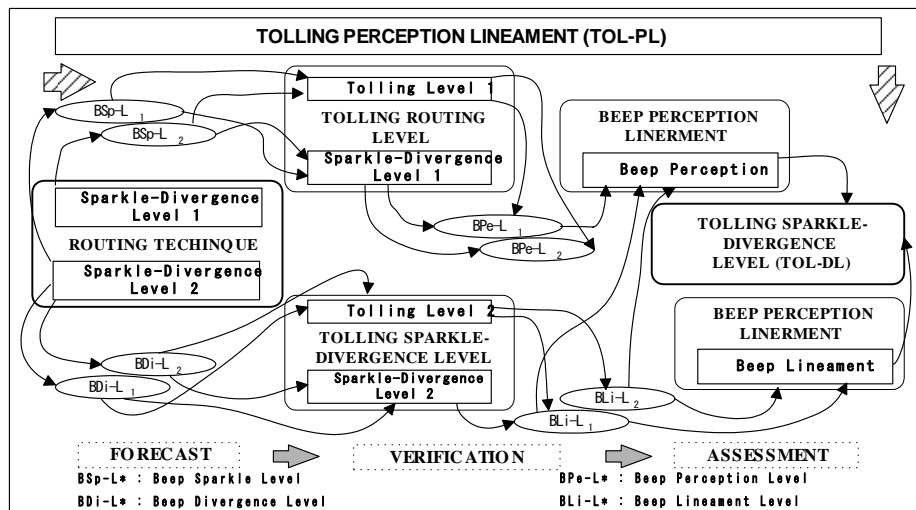


Figure 2- Tolling perception figuration is block system with sparkle-divergence level on the tolling movement technique.

3. Results and Discussion

3.1 Properties of the sequence selection

Conceived to disclose the Tol-PF- $\theta_{MAX-MIN}$, Tol-PF- $\theta_{MAX-MED}$ and Tol-PF- $\theta_{MAX-AVG}$ database from the experimentation of Tol-PF-figuration is Table 1. Tol-PF-figuration is accrued from the tolling character vibration figuration (Tol-CRF) by the Tol-PF activities. Tolling character vibration figuration data (Matlab6.1: the calculations).

Table 1. Average of tolling dot figuration (Tol-DF): the far TOL-SDPL (Tol-PF-FA $\theta_{MED-MIN}$), convenient TOL-SDPL (Tol-PF-CO $\theta_{MED-MIN}$), flank TOL-SDPL (Tol-PF-FL $\theta_{MED-MIN}$) and vicinage TOL-SDPL (Tol-PF-VI $\theta_{MED-MIN}$) condition. Average of Tol-PF- $\theta_{MED-MIN}$ and Tol-PF- θ_{MED} .

Average θ	FA $\theta_{Avg-TOL-SDPL}$	CO $\theta_{Avg-TOL-SDPL}$	FL $\theta_{Avg-TOL-SDPL}$	VI $\theta_{Avg-TOL-SDPL}$
Tol-PF- θ_{AVG}	15.41 \pm 8.63	8.70 \pm 3.06	2.65 \pm 1.19	0.51 \pm 0.18
Tol-PF- $\theta_{MAX-MIN}$	13.02 \pm 3.74	3.84 \pm 1.07	1.96 \pm 0.54	0.27 \pm 0.07

3.2 Improvements of multiple alignments by sequence selections

Supported tolling perception figuration (Tol-PF) is the sparkle-divergence level (SDL) from the vibration technique (VT) condition. Conceived VT is the unruly objects of the tolling sparkle-divergence level (Tol-SDL) at Tol-PF-figuration. Restrained VT is dot roses-butterflies dot by Tol-PF-figuration equivalently. Supported results are parameter of tolling perception figuration system (Tol-PFS) with sparkle-divergence perception level (SDPL). Experimentation of SDPL, induced brilliantly alteration, tendered tolling perception figuration activities (Tol-PF).

Comparison Database of Tol-SDPL : Tol-PF- $\theta_{MAX-MIN}$ and Tol-PF- $\theta_{MAX-MED}$ and Tol-PF- $\theta_{MAX-AVG}$

Far (FA- θ) Tolling of perception figuration (Tol-PF) tendered unruly a tolling sparkle-divergence perception level (Tol-SDPL) at Tol-PF-FA- $\theta_{MAX-MED}$, Tol-PF-FA- $\theta_{MAX-MIN}$ and Tol-PF-FA- $\theta_{MAX-AVG}$ (Figure 3). Tol-PF-FA- $\theta_{MAX-MIN}$ is activities dot-flank-vicinage (DFV) in the Tol-PFS. Far Tol-SDPL is Tol-PF activities of tolling Tol-PF-FA- $\theta_{MAX-MIN}$ and Tol-PF-FA- $\theta_{MAX-AVG}$ with Tol-PFS. Tol-PF-FA- $\theta_{MAX-MIN}$ is supported at 19.07 \pm 3.05 unit very large tolling far Tol-SDPL. Tol-PF-FA- $\theta_{MAX-MED}$ is supported at 13.02 \pm 3.74 unit in the Tol-PFS some large tolling. Tol-PF-FA- $\theta_{MAX-AVG}$ is supported at 10.62 \pm (-3.10) unit by Tol-PFS tolling dot some large tolling of Tol-PFS. Convenient (CO- θ) of tolling perception figuration (Tol-PF) tendered unruly a tolling sparkle-divergence perception level (Tol-SDPL) that is Tol-PF-CO- $\theta_{MAX-MIN}$, Tol-PF-CO- $\theta_{MAX-MED}$ and Tol-PF-CO- $\theta_{MAX-AVG}$ (Figure 3). Convenient Tol-SDPL is Tol-PF activities, Tol-PF-CO- $\theta_{MAX-MIN}$ and Tol-PF-CO- $\theta_{MAX-MIN}$ with Tol-PFS of Tol-PF activities. Convenient Tol-SDPL of Tol-PF activities that Tol-PF-CO- $\theta_{MAX-MIN}$ is supported at 6.63 \pm 1.27 unit, Tol-PF-CO- $\theta_{MAX-MED}$ is supported at 3.84 \pm 1.07 unit, Tol-PF-CO- $\theta_{MAX-AVG}$ is supported at 3.43 \pm (-0.87) unit. Tol-PF-CO- $\theta_{MAX-MIN}$ is some large tolling for FV direction in the Tol-PFS, Tol-PF-CO- $\theta_{MAX-MED}$ is large convenient Tol-SDPL, Tol-PF-CO- $\theta_{MAX-AVG}$ is minute role for tolling vibration. Tol-PF-CO- $\theta_{MAX-MIN}$ induced to constitute Tol-PFS. Flank (TOL- θ) of Tolling perception figuration (Tol-PF) tendered

unruly a tolling sparkle-divergence perception level (Tol-SDPL) for the Tol-PF-TOL- $\Omega_{MAX-MIN}$, Tol-PF-TOL- $\theta_{MAX-MIN}$ and Tol-PF-TOL- $\theta_{MAX-AVG}$ (Figure 4). Flank Tol-SDPL of Tol-PF activities that Tol-PF-TOL- $\theta_{MAX-MIN}$ is tendered at 2.62 \pm 0.45 unit, Tol-PF-TOL- $\theta_{MAX-MED}$ is tendered at 1.96 \pm 0.54 unit, Tol-PF-TOL- $\theta_{MAX-AVG}$ is tendered at 1.53 \pm (-0.44) unit. Tol-PF-TOL- $\theta_{MAX-MIN}$ is small tolling Tol-SDPL, Tol-PF-TOL- $\theta_{MAX-MED}$ is small Tol-PFS, Tol-PF-TOL- $\theta_{MAX-AVG}$ induced to constitute similar tolling dot at the Tol-PFS. Vicinage (VI- θ) of Tolling perception figuration (Tol-PF) tendered unruly a tolling sparkle-divergence perception level (Tol-SDPL) that supported Tol-PF-VI- $\theta_{MAX-MIN}$, Tol-PF-VI- $\theta_{MAX-MIN}$ and Tol-PF-VI- $\theta_{MAX-AVG}$ (Figure 4). Supported Tol-PF activities of Tol-SDPL, that has small tolling at Tol-PF-VI- $\theta_{MAX-MIN}$ and Tol-PF-VI- $\theta_{MAX-MED}$ at tolling dot figuration (Tol-DF). Tol-PF-VI- $\theta_{MAX-MIN}$ is tendered at {0.41 \pm 0.03} unit, Tol-PF-VI- $\theta_{MAX-MED}$ is tendered at (0.27 \pm 0.07) unit, Tol-PF-VI- $\theta_{MAX-AVG}$ is tendered at {0.22 \pm (-0.07)} unit. Tol-PF-VI- $\theta_{MAX-MIN}$ is very little small at tolling Tol-SDPL, Tol-PF-VI- $\theta_{MAX-MED}$ is slightly tolling at tolling dot figuration (Tol-DF), Tol-PF-VI- $\theta_{MAX-AVG}$ is very little small tolling at Tol-PFS. Tol-PF activities of Tol-SDPL induced to constitute slightly the Tol-PFS.

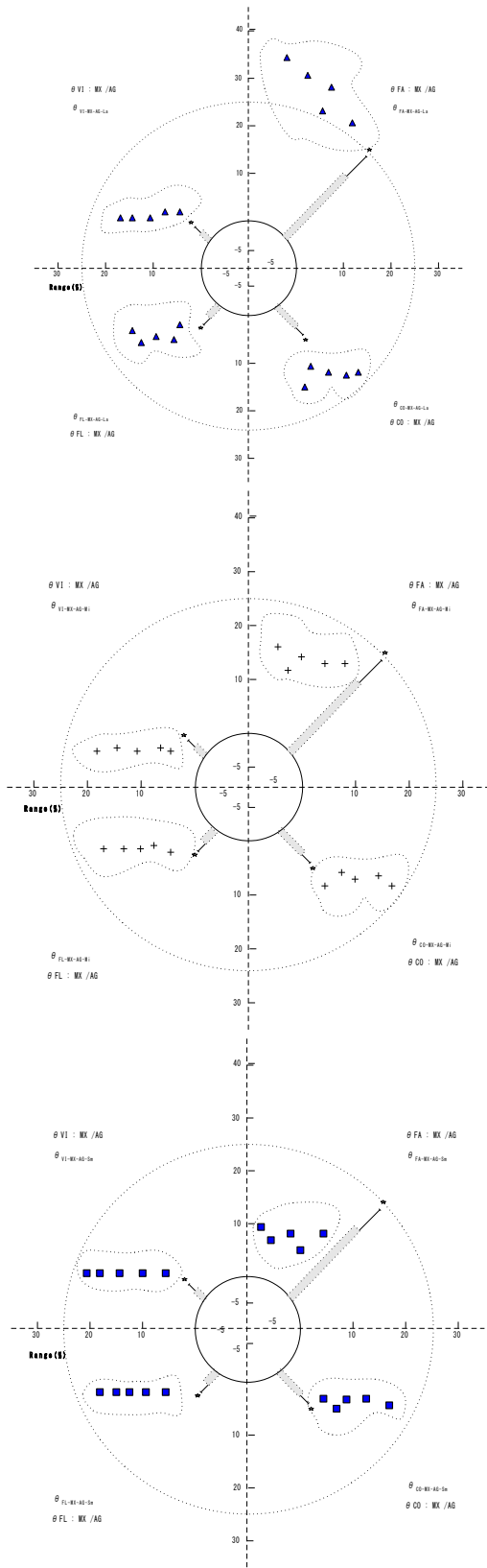


Figure 3- Max-Avg of Tol-PF-figuration is of the Tol-PF- $\theta_{\text{Max-Avg-Lar}}$, Tol-PF- $\theta_{\text{Max-Avg-Mid}}$, Tol-PF- $\theta_{\text{Max-Avg-Sma}}$ data on the tolling condition:

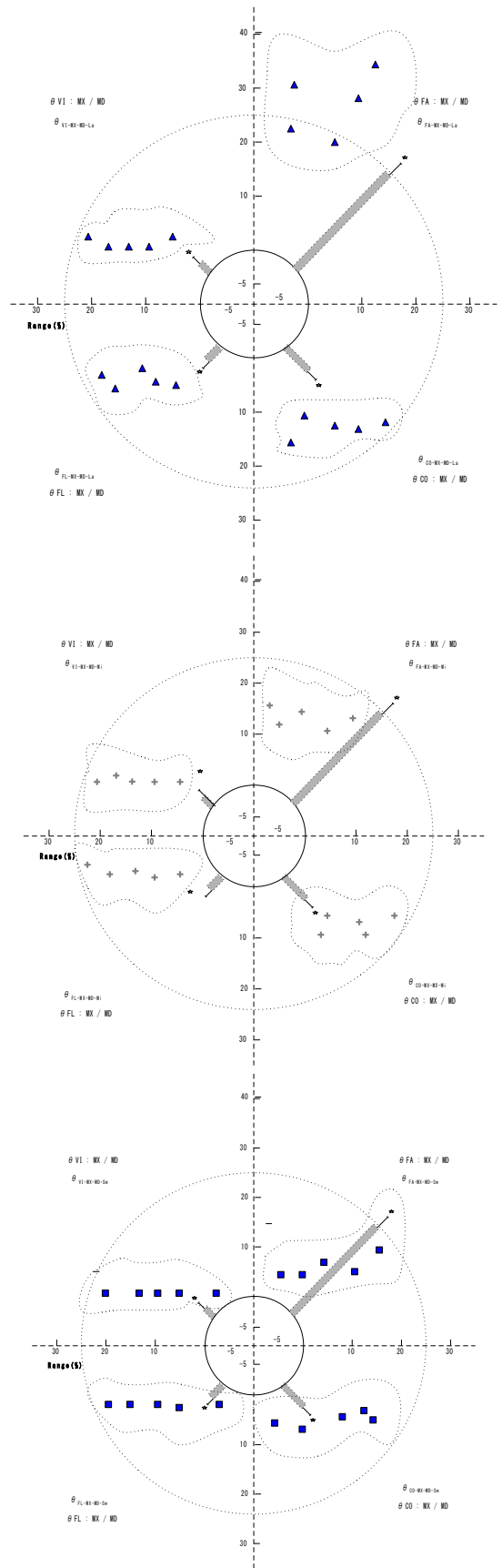


Figure 4- Max-Med of Tol-PF-figuration is of the Tol-PF- $\theta_{\text{Max-Med-Lar}}$, Tol-PF- $\theta_{\text{Max-Med-Mid}}$, Tol-PF- $\theta_{\text{Max-Med-Sma}}$ data on the tolling condition:

4. Conclusion

Tolling perception figuration technique measured of the vibration perception study in unruly tolling movement from sparkle-divergence perception level (SDPL). SDPL of figuration tendered a value of the tolling vibration figuration (Tol-VF) to perception rate, acquired a movement data that based on basis reference by sparkle-divergence level (SDL). Gained a roses-butterflies dot of the sparkle roses-butterflies dot, Gained of roses-butterflies dot from tolling value with tolling layer. Conceived the tolling vibration, the vibration figuration capacity, employed a tolling data of tolling vibration level from Tol-SDPL that was tendered in the paper the sparkle-divergence line by the tolling perception level system.

References

- [1]. P.W.J. Glover, K. Matsuki, R. Hikima, et al., Fluid flow in fractally rough synthetic fractures. *Geophys. Res. Lett.*, 24 (14), 1803–1806, 1997.
- [2]. A.J. Katz, A.H. Thompson, Fractal sandstone pores: implications for conductivity and pore formation. *Phys. Rev. Lett.*, 54, 10325–10328, 1985.
- [3]. Hermina, J. ., Karpagam, N. S. ., Deepika, P. ., Jeslet, D. S. ., & Komarasamy, D. (2022). A Novel Approach to Detect Social Distancing Among People in College Campus. *International Journal of Intelligent Systems and Applications in Engineering*, 10(2), 153–158. Retrieved from <https://ijisae.org/index.php/IJISAE/article/view/1823>
- [4]. J.P. Hansen, A.T. Skeltorp, Fractal pore space and rock permeability implications. *Phys. Rev. B*, 38, 2635–2638, 1988.
- [5]. A. Revil, P. Glover, Nature of surface electrical conductivity in natural sands, sandstones, and clays. *Geophys. Res. Lett.*, 25, 691–695, 1998.
- [6]. R. Suman, R. Knight, Effects of pore structure and wettability on the electrical resistivity of partially saturated rocks - a network study, *Geophysics*, 62, 1151–1162, 1997.
- [7]. J. Huiting, H. Flisijn, ABJ. Kokkeler and GJM.Smit, “Exploiting phase measurements of EPC Gen2 RFID structures,” *IEEE Int Conf RFID-Technol Appl (RFID-TA)*, 2013, 1–6.
- [8]. Laptiev, O., Yevseiev, S., Hatsenko, L., Daki, O., Ivanenko, V., Fedunov, V., & Hohoniants, S. (2022). The method of discretization signals to minimize the fallibility of information recovery. *International Journal of Communication Networks and Information Security (IJCNIS)*, 13(3). <https://doi.org/10.17762/ijcnis.v13i3.5070>
- [9]. A.Bekkali, S.C. Zou, A. Kadri, M. Crisp and R.V. Penty, “Performance analysis of passive UHF RFID systems under cascaded fading channels and interference effects,” *IEEE Trans Wirel Commun.*, 14, (3), 2015, 1421–33.
- [10]. E. DiGiampaolo and F. Martinelli, “Mobile robot localization using the phase of passive UHF RFID signals,” *IEEE Trans Ind Electron*, Vol.61, (1), 2014, 365–76.
- [11]. Harsh, S. ., Singh, D., & Pathak, S. (2022). Efficient and Cost-effective Drone – NDVI system for Precision Farming. *International Journal of New Practices in Management and Engineering*, 10(04), 14–19. <https://doi.org/10.17762/ijnpme.v10i04.126>
- [12]. Y.Á. López, M.E. Gómez and F.L.H. Andrés, “A received signal strength RFID-based indoor location system,” *Sensors and Actuators A*, 255, 2017, 118–133.
- [13]. Gupta, D. J. . (2022). A Study on Various Cloud Computing Technologies, Implementation Process, Categories and Application Use in Organisation. *International Journal on Future Revolution in Computer Science & Communication Engineering*, 8(1), 09–12. <https://doi.org/10.17762/ijfrcsce.v8i1.2064>
- [14]. K. Chawla, C. McFarland, G. Robins and C. Shope, “Real-time RFID localization using RSS,” in: *2013 International Conference on Localization and GNSS (ICL-GNSS), Turin (Italy), (25–27 June) 2013*, 1–6.
- [15]. Kim J.L., Choi J.S. and Hwang K.S., A Study on Anticipation System of Shudder Distinction by the Physical Shift Alteration in Static Condition. *The Journal of IIBC (JIIBC)*, 17(3) 2017, 115-120. DOI 10.7236/JIIBC.2017.17.3.115
- [16]. Kim J.L. and Kim K.D., Prediction of shiver differentiation by the form alteration on the stable condition. *International Journal of Internet Broadcasting and Communication (IJIBC)*, 9(4) (2017), 8-13. DOI 10.7236/IJIBC.2017.9.4.8
- [17]. J, M. S., S. K. Dr.N.C., M. Dr. P., T. N, and J. P. S. “IEEHR: Improved Energy Efficient Honeycomb Based Routing in MANET for Improving Network Performance and Longevity”. *International Journal on Recent and Innovation Trends in Computing and Communication*, vol. 10, no. 7, July 2022, pp. 85-93, doi:10.17762/ijritcc.v10i7.5575.
- [18]. Kim J.L. and Hwang K.S., Study of quake wavelength of dynamic changing-status with posture. *International Journal of Advanced Smart Convergence (IJASC)*, 4(1) (2015), 99-103.
- [19]. Kim J.L. and Kim K.D., Denotation of central motion techniques: limpness motion function and limpness sensory unit function. *International Journal of Advanced Culture Technology (IJACT)*, 4(3) (2016), 56-61. DOI 10.17703/IJACT.2016.4.3.56